ELSEVIER

Biophysical Chemistry 90 (2001) 17–30

Biophysical Chemistry

www.elsevier.nl/locate/bpc

Birhythmicity, trirhythmicity and chaos in bursting calcium oscillations

Thomas Haberichter[a,*], Marko Marhl[b], Reinhart Heinrich[a]

[a] *Humboldt University Berlin, Institute of Biology, Theoretical Biophysics, Invalidenstr. 43, D-10115 Berlin, Germany*
[b] *University of Maribor, Faculty of Education, Department of Physics, Koroška cesta 160, 2000 Maribor, Slovenia*

Received 11 September 2000; received in revised form 12 December 2000; accepted 15 December 2000

Abstract

We have analyzed various types of complex calcium oscillations. The oscillations are explained with a model based on calcium-induced calcium release (CICR). In addition to the endoplasmic reticulum as the main intracellular Ca^{2+} store, mitochondrial and cytosolic Ca^{2+} binding proteins are also taken into account. This model was previously proposed for the study of the physiological role of mitochondria and the cytosolic proteins in gene rating complex Ca^{2+} oscillations [1]. Here, we investigated the occurrence of different types of Ca^{2+} oscillations obtained by the model, i.e. simple oscillations, bursting, and chaos. In a bifurcation diagram, we have shown that all these various modes of oscillatory behavior are obtained by a change of only one model parameter, which corresponds to the physiological variability of an agonist. Bursting oscillations were studied in more detail because they express birhythmicity, trirhythmicity and chaotic behavior. Two different routes to chaos are observed in the model: in addition to the usual period doubling cascade, we also show intermittency. For the characterization of the chaotic behavior, we made use of return maps and Lyapunov exponents. The potential biological role of chaos in intracellular signaling is discussed.

Keywords: Complex calcium oscillations; Bursting; Chaos; Intermittency

* Corresponding author. Tel.: +49-30-2093-8698; fax: +49-30-2093-8813.
E-mail address: mail@thabe.de (T. Haberichter).

0301-4622/01/$ - see front matter
PII: S0301-4622(01)00127-2

1. Introduction

Many processes in excitable as well as in non-excitable cells are controlled by the oscillatory changes of cytosolic calcium concentration. Calcium oscillations were found experimentally in the 1980s [2,3], and numerous experimental works have confirmed their important physiological role in cell signaling [4,5]. To explain the mechanism of Ca^{2+} oscillations, many theoretical studies have been carried out [[6–15]; for review see [4]]. It is widely agreed that the endoplasmic reticulum (ER) represents the main calcium store, which plays a predominant role in generating the intracellular Ca^{2+} oscillations. In some theoretical studies, other intracellular Ca^{2+} stores were also considered. Most often the Ca^{2+}-binding cytosolic proteins are included in the models explaining Ca^{2+} oscillations [12–17]. Recently, it has become more and more clear that mitochondria also play an important role in intracellular calcium signaling (for example, cf. [18]). Surprisingly, in comparison to the huge number of experimental evidences about mitochondrial importance in intracellular calcium signaling [18–30], rather few theoretical studies take it into account [6,13,31,32].

Most theoretical works explaining the mechanism of Ca^{2+} oscillations are concerned with simple Ca^{2+} oscillations, i.e. oscillations that have the form of sharp spikes with a constant amplitude and a well defined frequency. However, in experiments, very often more complex forms of calcium oscillations can be observed as well (for review, see [33]). The most usual type of such complex oscillations is represented by a periodic succession of a silent, relatively quiescent, and an active phase, during which the system exhibits rapid oscillations. This type of oscillation is called *bursting* and is better known in the case of electrical bursting (e.g. [34]; for review see [35]). The mathematical analysis of a model bursting neuron R15 in Applysia originally proposed by Canavier et al. [36] has been carried out by Butera [37]. He considers a model of four variables. Two of these variables operate on a time scale much slower than the remaining ones, which allows the employment of a geometric approach, introduced by Rinzel and Lee [38], to explain the origin of bursting and multirhythmicity.

In the field of intracellular calcium signaling, bursting is studied to a lesser extent. Firstly, the theoretical analysis of a mechanism for bursting Ca^{2+} oscillations has been carried out by Shen and Larter [39]. A more detailed study of different mechanisms explaining the complex Ca^{2+} oscillations in non-excitable cells have been given by Borghans et al. [33] and further mathematically analyzed by Houart et al. [40]. Another model revealing bursting oscillations was proposed by Kummer et al. [41]. Usually, the mechanism explaining the complex Ca^{2+} oscillations is related to the open fraction of the Ca^{2+}-release channels in the ER. In some approaches, this is explicitly the consequence of changes in $InsP_3$ production, which has a direct influence on the opening probability of the $InsP_3$-sensitive calcium channels in the ER [42]. In a previous paper [1], we have proposed another mechanism for the generation of complex intracellular calcium oscillations based on calcium exchange between different Ca^{2+} stores in the cell. In addition to the ER as the main intracellular Ca^{2+} store, Ca^{2+} sequestration in the mitochondria and Ca^{2+} binding to cytosolic proteins are taken into account.

The aim of the present study was to analyze in more detail the occurrence of various types of complex Ca^{2+} oscillations. We used the model that was previously proposed for the study of the physiological role of mitochondria and cytosolic proteins in generating complex Ca^{2+} oscillations [1]. The model offers a good opportunity for the mathematical analysis of complex Ca^{2+} oscillations because it leads to a large number of different oscillatory modes. In addition, the whole spectrum of the different types of complex Ca^{2+} oscillations was obtained by changing only one model parameter, which corresponds to physiological variations of extracellular agonists such as hormones or neurotransmitters. Thus, it is rather suggestive to use this quantity as a bifurcation parameter in the mathematical analysis. It was demonstrated that a single bifurcation diagram suffices to show many various types of complex Ca^{2+} oscillations, from simple oscillations to bursting and chaos.

Bursting Ca^{2+} oscillations are focussed on in particular, because they appear in different forms, from simple to folded limit cycles and chaos. All different types of bursting oscillations show a number of common properties. The amplitudes of cytosolic calcium concentration remain almost constant over the whole range of the bifurcation parameters, even in the chaotic mode. Further, the oscillation frequencies (which, in the case of folded or chaotic oscillations, have to be understood as average frequencies, with respect to the main peaks of cytosolic Ca^{2+}) remain similar for slight changes of the bifurcation parameter, no matter if there is a bifurcation between them. The system shows birhythmic and trirhythmic behaviors. Here, we have used these terms to express that two and three different limit cycles, respectively, may occur at the same value of the bifurcation parameter. This has to be distinguished from the more general *bi- (tri-)stability*: the coexistence of two (three) stable solutions, where typically one solution is in equilibrium and the other(s) is (are) periodic. These limit cycles differ slightly in their forms and are, in part, also differently folded. Chaotic behavior is obtained in several separated intervals of the above mentioned bifurcation parameter. It is characterized by calculating the largest Lyapunov exponent. Two different transitions to the chaotic regimes have been found. In addition to the most typical *period doubling cascade*, this is the so-called *intermittency route to chaos*.

In Section 2, the mathematical model is shortly introduced with a schematic presentation and the complete set of model equations and parameter values. Section 3 contains the mathematical analysis of the various types of complex Ca^{2+} oscillations. First, the occurrence of the different oscillatory modes is presented by a bifurcation diagram and, subsequently, the phenomena of bursting, birythmicity, trirhythmicity and chaotic Ca^{2+} oscillations are studied in some more detail. In Section 4, the results and model predictions are evaluated and compared with experimental data and other theoretical works in the field. At the end, the potential biological role of complex Ca^{2+} oscillations and, in particular, the hypothetical physiological importance of chaotic Ca^{2+} oscillations in intra- and intercellular signaling is discussed.

2. Model

We used the model system that we have previously proposed for studying the physiological role of mitochondria and the cytosolic proteins in generating complex Ca^{2+} oscillations [1]. Here, we present a summary of the relevant processes and the model equations. The model is shown schematically in Fig. 1. It describes the exchange of calcium between the cytosol and three different calcium stores: the ER, mitochondria, and calcium binding proteins in the cytosol. Calcium

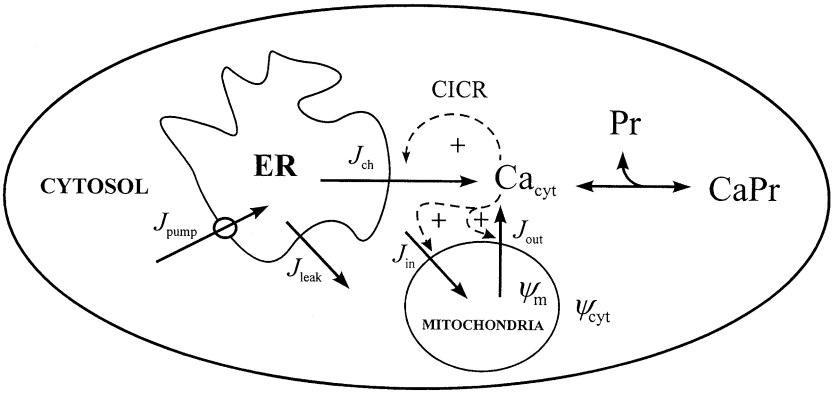

Fig. 1. Schematic presentation of the model system.

fluxes through the cell membrane are neglected. Between the cytosol and the ER, three different calcium fluxes are considered: ATP-dependent calcium uptake from the cytosol into the ER (J_{pump}) and calcium leak flux from the ER into the cytosol (J_{leak}) are both taken as linear functions. The calcium flux from the ER into the cytosol (J_{ch}) follows the calcium-induced calcium release (CICR) mechanism. This positive feedback is taken into account by a sigmoid dependency of the flux rate with respect to the cytosolic calcium concentration. Mitochondrial calcium is increased by active calcium uptake from the cytosol by mitochondrial uniporters (J_{in}). Due to experimental evidence, the uniporters are taken as an 'almost stepwise' function of Ca_{cyt}. From the mitochondria into the cytosol, we consider a very small non-specific leak flux (J_{out}), which is taken as a linear function of Ca_m. Further, we include calcium release into the cytosol through Na^+/Ca^{2+} exchangers combined with a flux through mitochondrial permeability transition pores (PTPs) in a very low-conductance state. There is little evidence for this mechanism [24,43,44], and the quantification of the parameters is difficult. We included this term for the sake of generality. Exchanging it for a linear term with a suitable constant does not alter the model predictions.

Two conservation relations for the total cellular calcium concentration (Ca_{tot}) and the total concentration of bound and unbound proteins (Pr_{tot}) are applied:

$$Pr_{tot} = CaPr + Pr \tag{1}$$

$$Ca_{tot} = Ca_{cyt} + \frac{\rho_{ER}}{\beta_{ER}} Ca_{ER} + \frac{\rho_m}{\beta_m} Ca_m + CaPr. \tag{2}$$

Here ρ_{ER} and ρ_m represent the volume ratio between the ER and the cytosol and between the mitochondria and the cytosol, respectively. Assuming very fast unsaturated buffering of Ca^{2+} in the ER and mitochondrial compartments, we use constant factors β_{ER} and β_m for relating the concentrations of free calcium in the ER and the mitochondria to their respective total concentrations. This reduces the number of variables from five to three, describing the free concentration of calcium ions in the cytosol (Ca_{cyt}), in the ER (Ca_{ER}), and in the mitochondria (Ca_m). Denoting the concentration of free Ca^{2+} binding sites on the cytosolic proteins by Pr, the concentration of bounded Ca^{2+} binding sites on the cytosolic proteins by $CaPr$, the model equations read:

$$\frac{dCa_{cyt}}{dt} = J_{ch} + J_{leak} - J_{pump} + J_{out} - J_{in} + k_{-}CaPr - k_{+}Ca_{cyt}Pr \tag{3}$$

$$\frac{dCa_{ER}}{dt} = \frac{\beta_{ER}}{\rho_{ER}}(J_{pump} - J_{ch} - J_{leak}) \tag{4}$$

$$\frac{dCa_m}{dt} = \frac{\beta_m}{\rho_m}(J_{in} - J_{out}) \tag{5}$$

The different fluxes are given as:

$$J_{ch} = k_{ch}\frac{Ca_{cyt}^2}{K_1^2 + Ca_{cyt}^2}(Ca_{ER} - Ca_{cyt}) \tag{6}$$

$$J_{leak} = k_{leak}(Ca_{ER} - Ca_{cyt}) \tag{7}$$

$$J_{pump} = k_{pump}Ca_{cyt} \tag{8}$$

$$J_{out} = \left(k_{out}\frac{Ca_{cyt}^2}{K_1^2 + Ca_{cyt}^2} + k_m\right)Ca_m \tag{9}$$

$$J_{in} = k_{in}\frac{Ca_{cyt}^8}{K_2^8 + Ca_{cyt}^8} \tag{10}$$

Model parameters used in our calculations are listed in Table 1. Most of the parameter values are taken from measurements reported in the literature. For more detailed discussions the reader may consult our previous papers [1,12–14].

3. Results

The model Eqs. (1)–(10) were integrated

Table 1
Model parameters for which all results are calculated unless otherwise stated

Parameter		Value
Total concentrations		
Ca_{tot}	total cellular Ca^{2+} concentration	90 μM
Pr_{tot}	total concentration of cytosolic proteins	120 μM
Geometric parameters		
ρ_{ER}	volume ratio between the ER and the cytosol	0.01
ρ_m	volume ratio between the mitochondria and the cytosol	0.01
β_{ER}	ratio of free Ca^{2+} to total Ca^{2+} in the ER	0.0025
β_m	ratio of free Ca^{2+} to total Ca^{2+} in the mitochondria	0.0025
Kinetics parameters		
k_{ch}	maximal rate constant of Ca^{2+} channels in the ER membrane	4100 s^{-1}
k_{pump}	rate constant of ATP-ases	20 s^{-1}
k_{leak}	rate constant of Ca^{2+} leak flux through the ER membrane	0.05 s^{-1}
k_{in}	maximal rate constant of uniporters in the mitochondrial membrane	300 μM s^{-1}
k_{out}	maximal rate for Ca^{2+} flux through Na^+/Ca^{2+} exchangers and PTPs	125 s^{-1}
k_m	rate constant of the non-specific leak flux	0.00625 s^{-1}
k_+	on rate constant of Ca^{2+} binding to proteins	0.1 μM^{-1} s^{-1}
k_-	off rate constant of Ca^{2+} binding to proteins	0.01 s^{-1}
K_1	half saturation for Ca^{2+}	5 μM
K_2	half saturation for Ca^{2+} of uniporters in the mitochondrial membrane	0.8 μM

numerically for fixed parameter values listed in Table 1. In the various simulations, only the parameter k_{ch}, the rate constant of the Ca^{2+} channels in the ER membrane, is changed. This quantity depends significantly on external stimuli, which makes it a good candidate for bifurcation analysis, because it is accessible through experiments. The oscillatory regime extends from $k_{ch} = 473\ s^{-1}$ to $k_{ch} = 4603\ s^{-1}$. In Fig. 2, the time courses of Ca_{cyt} and Ca_m are illustrated for three examples of these oscillations: simple spike-like oscillations at $k_{ch} = 1100\ s^{-1}$, two different modes of bursting oscillations at $k_{ch} = 3500\ s^{-1}$, achieved by using different initial values. Note that the maxima of Ca_{cyt} are nearly identical. In contrast, the maxima of Ca_m differ much more.

In Fig. 3 the bifurcation diagram for a part of the oscillatory region ($k_{ch} = 1800\ s^{-1}$ to $k_{ch} = 4100\ s^{-1}$) is presented. In the diagram, we show only the maxima of mitochondrial calcium concentration Ca_m. We chose this variable in favor of the cytosolic calcium concentration Ca_{cyt}, because the amplitude of the latter remains almost the same, at different values of k_{ch} as well as at different phases of the complex oscillations analyzed. For small values of k_{ch} simulation leads to simple spike-like oscillations. At $k_{ch} = 1800\ s^{-1}$ the system shows, in addition to the spike, slight variations of cytosolic calcium on top of a plateau level, which initiates the transition into the regime of bursting oscillations, which extends until $k_{ch} = 4500\ s^{-1}$, where a transition back to simple oscillations takes place.

In this work, we have concentrated on bursting calcium oscillations. In part A of the bifurcation diagram, these oscillations occur only as simple limit cycle oscillations, here called *simple bursting*. In contrast to simple spike-like oscillations, in this case the well-expressed main maximum of cytosolic Ca^{2+} is followed by several maxima of lower amplitude. Note that in this case, only the main maxima are plotted in Fig. 3. Further intervals of simple bursting include parts C and E.

A more complex form of bursting oscillations corresponds to double folded limit cycles. An example of this oscillatory mode occurs in regime B (cf. inset I of Fig. 3). The two crosshatched lines represent two main Ca_m maxima of the

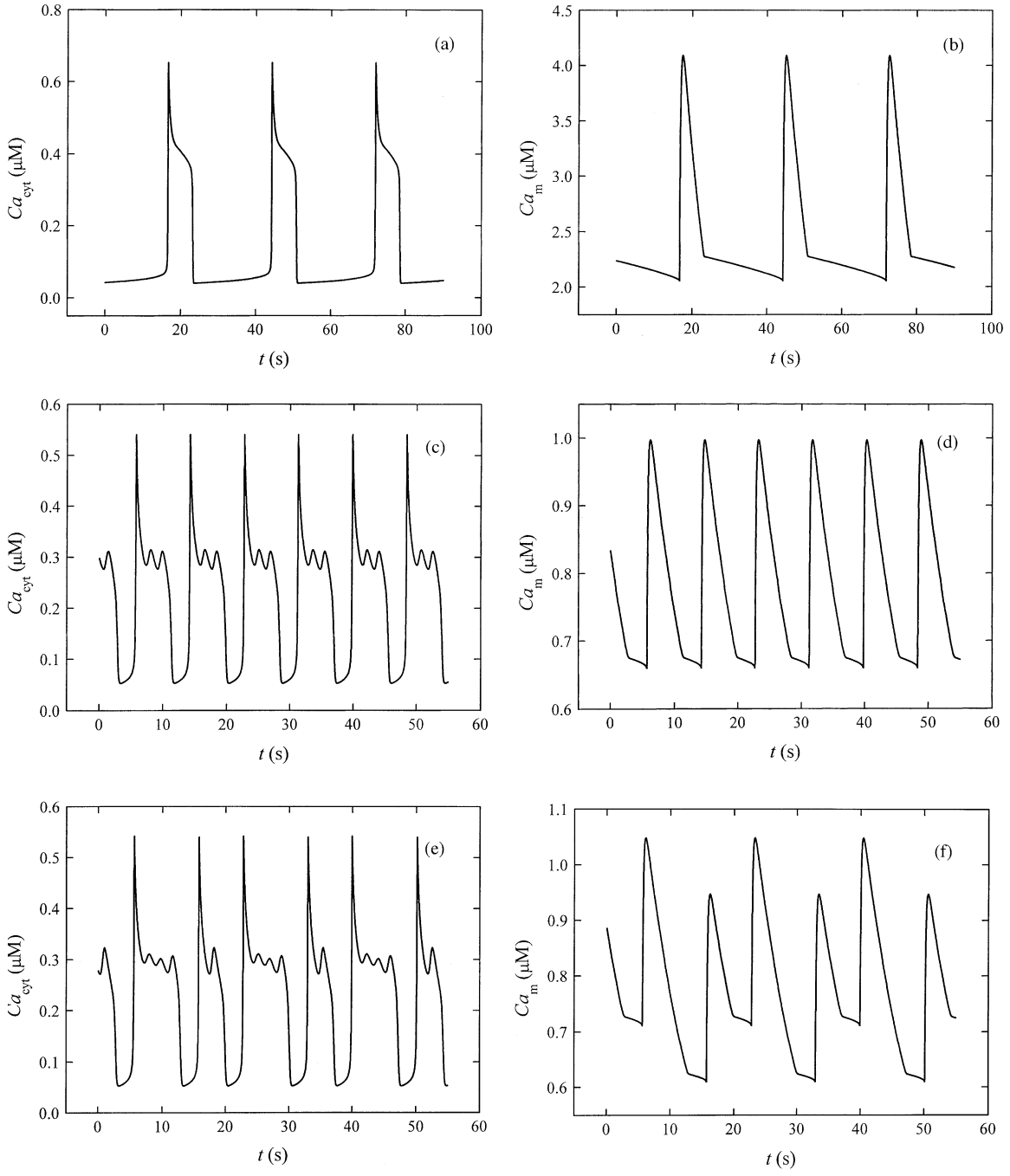

Fig. 2. Time courses of cytosolic Ca^{2+} concentration. (a) $k_{ch} = 1100\ s^{-1}$, (c) $k_{ch} = 3500\ s^{-1}$, unfolded solution for initial conditions ($Ca_{cyt} = 0.1\ \mu M$, $Ca_{ER} = 1.0\ \mu M$, $Ca_m = 0.65\ \mu M$), (e) $k_{ch} = 3500\ s^{-1}$, folded solution for initial conditions ($Ca_{cyt} = 0.1\ \mu M$, $Ca_{ER} = 1.0\ \mu M$, $Ca_m = 1.0\ \mu M$). (b), (d), and (f) represent the respective time courses of mitochondrial Ca^{2+}.

folded limit cycle, which consists of two similar parts of the full trajectory, called *bursting cycles*. Note that the full line corresponds to simple bursting oscillations, which occur in the same region. The complexity of bursting oscillations grows with a further folding of the limit cycle. In the middle of part G (c.f. inset II of Fig. 3) the system exhibits five-times folded limit cycles, which is demonstrated by five lines representing the five main Ca_m maxima of the five bursting cycles, appearing within one single limit cycle.

In certain parts of the bifurcation diagram, for example in part D between $k_{ch} = 2780\ s^{-1}$ and $k_{ch} = 2980\ s^{-1}$, and in part G, between $k_{ch} = 3598\ s^{-1}$ and $k_{ch} = 3636\ s^{-1}$, with several interruptions, the bursting calcium oscillations exhibit chaos. Period doubling cascades lead to the regimes of chaotic behavior in some parts of the bifurcation diagram. One example of such a transition can be realized in inset II at approximately $k_{ch} = 3600\ s^{-1}$. In some other parts of the diagram, e.g. at the threshold between parts D and E, another transition to chaos can be observed. This is referred to as *intermittency route to chaos*, which will be discussed below. For values of the bifurcation parameter exceeding those of part G, frequent changes between simple and folded limit cycles occur with chaotic regimes in-between. In Fig. 3 this is only shown up to $k_{ch} = 4100\ s^{-1}$.

Another dynamical feature of the system is characterized by an occurrence of two different limit cycles at the same value of the bifurcation parameter. This phenomenon is referred to as birhythmicity. In Fig. 3, we show such an occurrence of *birhythmicity* in the parameter range between $k_{ch} = 1968\ s^{-1}$ and $k_{ch} = 2456\ s^{-1}$ (part

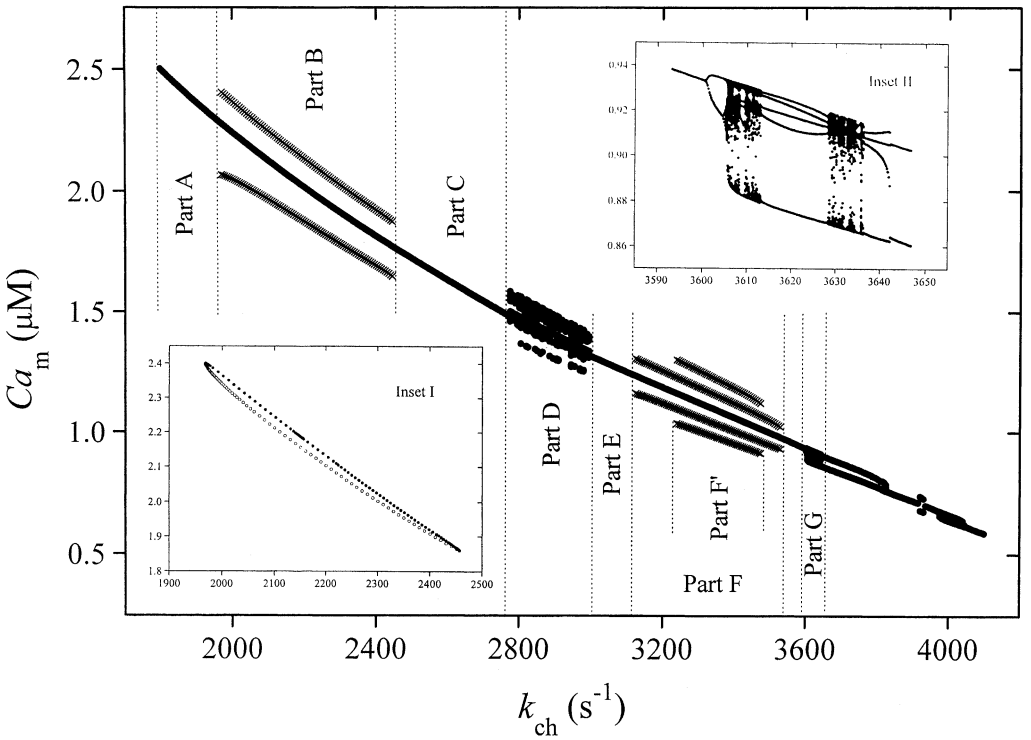

Fig. 3. Bifurcation diagram, showing the main maxima of Ca_m for k_{ch} between 1800 and 4100 s^{-1}. Simple bursting oscillations appear in parts A, C and E, birhythmicity in parts B and F, trirhythmicity in part F′, and chaos in parts D and G. In the cases of multirhythmicity, additional limit cycles are represented by crosses. Inset I shows the maxima of the stable and unstable limit cycles, which occur through a saddle node bifurcation in part B. Inset II is a detail magnification of part G.

B). Note that in this case, one of the limit cycles is double folded. Its two main maxima are represented by the crosses in part B of Fig. 3. The maxima of the unfolded limit cycles appear as a continuous line.

Also in part F of the bifurcation diagram, between $k_{ch} = 3120\ s^{-1}$ and $k_{ch} = 3534\ s^{-1}$, we get two different limit cycles for the same bifurcation parameter value. Additionally, in the subregion between $k_{ch} = 3225\ s^{-1}$ and $k_{ch} = 3480\ s^{-1}$ (part F′), a third limit cycle occurs for another set of initial conditions (trirhythmicity). One of them is unfolded, the other two limit cycles are double folded, so one continuous line and two pairs of crosses are plotted in the diagram.

3.1. Bursting

The bursting oscillations of cytosolic calcium concentration obtained by our model give a good reproduction of the typical experimental observations (cf. [33]). They are characterized by a sharp rise to a high level of Ca_{cyt}, followed by the active phase, in which the concentration of cytosolic calcium oscillates at an intermediate calcium level, with higher frequencies and lower amplitudes compared to the whole cycle. After an intermediate silent phase, the peak is reached again. This has already been presented in [1]. Let us now explain the occurrence of the active phase by considering one example of a simple limit cycle at $k_{ch} = 3500\ s^{-1}$, of which the time courses of Ca_{cyt} and Ca_m are depicted in Fig. 2c,d.

As can be seen in the stated figures, Ca_m declines with an almost constant rate during the active phase. At the same time, all other variables oscillate, i.e. they produce the activity. With the objective of understanding the system behavior during the active phase, it seems to be suitable to consider a reduced two-dimensional system in which the *non-active* variable Ca_m is turned into a parameter, although this method is not strictly justified as it is in the example of Rinzel et al. (cf. [45]). Also in contrast to the example of electrical bursting analyzed by Butera [37], in which the reduced model can predict bursting behavior a priori, here we can employ it to give an a posteriori explanation.

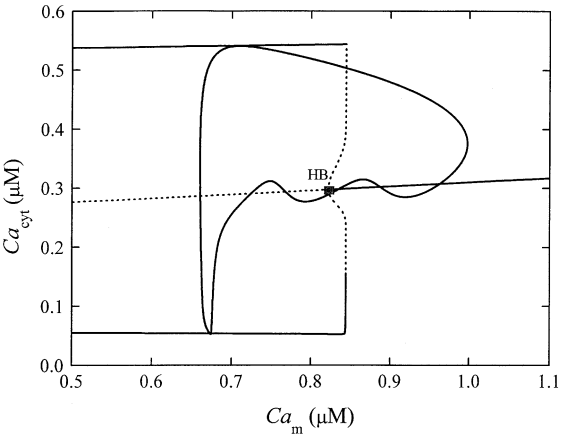

Fig. 4. Bifurcation diagram of the reduced two-dimensional system at $k_{ch} = 3500\ s^{-1}$, in which Ca_m is treated as bifurcation parameter. Unstable (dashed line) and stable steady states, as well as maxima and minima of limit cycle oscillations are depicted. HB stands for Hopf bifurcation. The closed line represents the unfolded limit cycle trajectory of the complete system. The respective time courses of Ca_{cyt} and Ca_m are those depicted in Fig. 2c,d.

The bifurcation diagram of this reduced system is depicted in Fig. 4. In addition to the stable and unstable steady states of Ca_{cyt}, the maxima and minima of the oscillatory solutions are plotted. In the same diagram, a projection of the limit cycle trajectory of the complete system is shown. The Hopf bifurcation at $Ca_m = 0.822\ \mu M$ is almost identical to the critical borderpoint between stable steady state behavior at higher Ca_m and stable limit cycle behavior at lower Ca_m.

In the reduced model, a Ca_m higher than the critical value results in a stable focus, i.e. the trajectory shows oscillations of declining amplitudes. In a similar way, damped oscillations of all variables excluding Ca_m are observed while Ca_m is high. As soon as Ca_m gets below the Hopf bifurcation point, the stable focus becomes unstable and the amplitude of Cacyt grows and reaches the limit cycle amplitude of the reduced system.

3.2. Birhythmicity and trirhythmicity

For a given value of k_{ch} within parts B and F of the bifurcation diagram (Fig. 3), the model

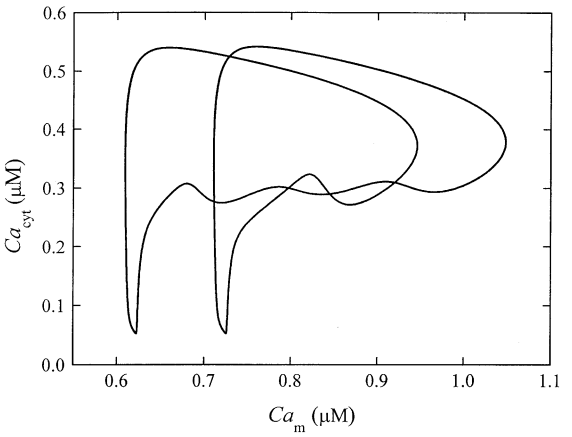

Fig. 5. Birhythmicity: folded limit cycle obtained by the same set of parameters, but different initial conditions than in Fig. 4. The respective time courses of Ca_{cyt} and Ca_m are those depicted in Fig. 2e,f.

system has more than one attractor. The trajectory tends to one of them, depending on the initial conditions. In the case of two attractors this phenomenon is called *birhythmicity*. For example, the limit cycle for $k_{ch} = 3500\ s^{-1}$ illustrated in Fig. 4 (see also Fig. 2c,d), is reached only if the simulation is started with certain initial conditions. For other initial conditions the system is attracted by the folded limit cycle shown in Fig. 5 (see also Fig. 2e,f).

The folded limit cycles, which exist in the cited intervals of the bifurcation diagram in addition to other limit cycles beyond those intervals, appear in a process which is similar to a saddle-node bifurcation in the case of stationary states, where a stable node and a saddle point appear simultaneously. Here, a stable and an unstable limit cycle appear. In inset I of Fig. 3, the stable folded limit cycles appearing in part B of the bifurcation diagram are represented by their largest maxima (filled circles). Note that the secondary peaks, which additionally appear in the bifurcation diagram (see the main part of Fig. 3), are not represented in the inset. The maxima of the unstable limit cycles, which appear the same time, are depicted as open circles.

From the mathematical point of view, the phenomenon of *trirhythmicity* can also be explained in an analogous way as the emergence of birhythmicity. It stands for the case of a coexistence of three different limit cycles that may attract the trajectories of the system. An example of this has been found in part F′ of Fig. 3. It should be stressed that further stable solutions of the model system might be found for any value of the bifurcation parameter k_{ch}. Hence, it is hard to complete the bifurcation diagram.

3.3. Chaotic bursting Ca^{2+} oscillations

There is a number of intervals for the bifurcation parameter in which the system shows chaotic behavior. With parts D and G, we have denoted the most extended ones. Inset II in the bifurcation diagram (Fig. 3) shows a magnification of the latter part. The chaotic behavior is characterized by a positive value of the largest Lyapunov exponent, e.g. for $k_{ch} = 2950\ s^{-1}$ it has been quantified as $\lambda = 0.014\ s^{-1}$. This has to be opposed to the calculation of the largest Lyapunov exponent of the simple limit cycle of $k_{ch} = 4100\ s^{-1}$, for example, which gives the expected zero value. Of special interest in the analysis of chaos are the transitions between limit cycles and chaotic behavior. In the present system, two different types of such transitions occur.

3.3.1. Period doubling

The first type of transition to chaos is characterized by the repetitive doubling of periods that comes along with continuous variation of the bifurcation parameter into the respective chaotic region. An example of a period doubling cascade is sketched in inset II of Fig. 3. Again, for the folded limit cycles all main maxima are plotted. Thus the number of lines/points for a given value of k_{ch} corresponds to the periodicity of the respective limit cycle, or expresses the chaotic behavior.

3.3.2. Intermittency

The second type of transition to chaos found in our system is known as an *intermittency route*. It is best visualized with the help of return maps. An appropriate return map is obtained by using a one-dimensional projection of a Poincaré section,

which is transpassed exactly once during each cycle. Fig. 6a shows such a return map for an example of intermittent behavior. The values of Ca_m at which the system trajectory crosses in a given direction the chosen Poincaré section (here $Ca_{cyt} = 0{:}15\ \mu M$) are referred to as x_n. Recording the trajectory for very long times yields a set of points that create segments of an almost continuous curve, which might be imagined as the graph of a function $f{:}x_n \mapsto x_n + 1$. The zig–zag line demonstrates the trajectory of these points during a limited time interval. The line passes through the narrow gap between the imaginative function f and the bisector line (see Fig. 6b). Each single point of the return map represents one cycle of the system trajectory. During the passage of the gap, the points on the return map remain almost constant. Consequently, the system trajectory maintains a very similar form for each cycle that these points represent. After leaving the gap at its lower left corner, the exact behavior is rather unpredictable. The curve leaves the gap *intermittently*, and the subsequent points $(x_n,\ x_n + 1)$ on the return map are rather distant from each other. As soon as the points $(x_n,\ x_n + 1)$ return to the upper right end of the gap the period of *almost constancy* restarts. Fig. 6c shows the time dependence of the subsequent x_n values over an ex-

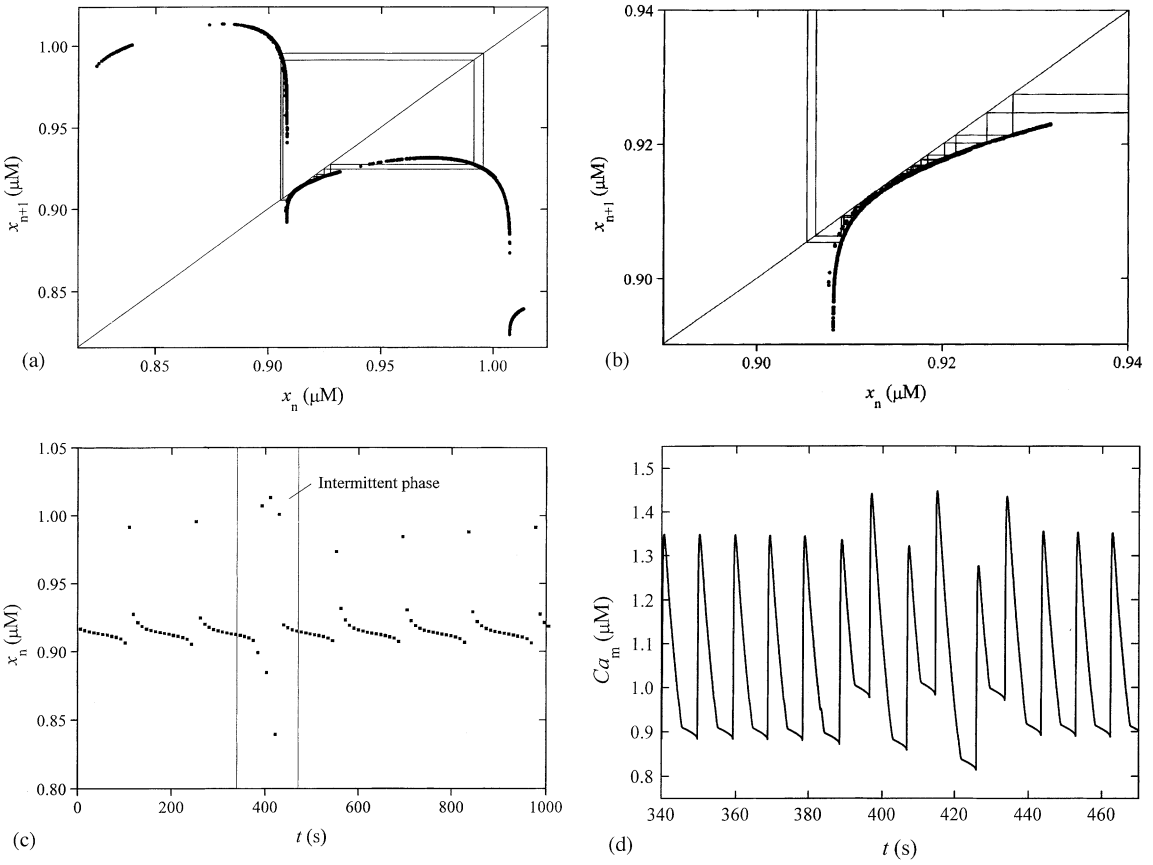

Fig. 6. Intermittent behavior at $k_{ch} = 2950\ s^{-1}$. (a) Return map showing the values x_n of Ca_m at which the system trajectory crosses the Poincaré section $Ca_{cyt} = 0{:}15\ \mu M$ vs. their respective predecessors. Additionally, the bisector line and a trajectory of subsequent x_n are depicted. (b) Detail magnification of (a). (c) Time course of x_n for an extended period of time. (d) Time course of Ca_m for the time interval highlighted in (c).

tended period of time. The interval highlighted in this figure (340 s $< t <$ 470 s) corresponds to the intermittent phase of which the time course of Ca_m is plotted in Fig. 6d. The term *intermittency route to chaos* can be explained most easily as the route out of chaos, i.e. when the bifurcation parameter is changed from the (intermittent) chaotic regime into the limit cycle regime. Then the set of return points — and thus the imaginative curve f — moves towards the bisector line, which leads to longer periods of *almost identical* cycles as the gap becomes more narrow. As the curve f, which corresponds to an imaginative discrete map, crosses the bisector line, one stable and one unstable steady state emerge at the intersection points with the bisector line. In our case, the trajectory approaches the limit cycle, which corresponds to one of the intersection points of the imaginative function f with the bisector line.

4. Discussion

In this paper, the bifurcation analysis of complex Ca^{2+} oscillations is carried out. We use the model previously proposed for the study of the physiological role of mitochondria and the cytosolic proteins in generating complex Ca^{2+} oscillations [1]. The model reveals a novel mechanism explaining complex oscillations of cytosolic calcium concentration. Moreover, it offers a good opportunity for a bifurcation analysis of complex Ca^{2+} oscillations because it explains a large number of different oscillatory modes, i.e. simple and bursting oscillations. The latter appear as simple or folded limit cycles and as chaotic attractors. In certain regions of the parameter space birhythmicity and trirhythmicity are observed. All these different types of complex calcium oscillations show a temporal pattern, which is also observed experimentally (for review, see [4,5]). Transients of cytosolic calcium obtained by the model have a typical spike-like form and reasonable frequencies and amplitudes. We emphasize that the amplitudes of the main calcium spikes remain nearly constant in the whole range of the oscillatory regime. As explained in a previous publication [13], the constancy of amplitudes of calcium oscillations is a consequence of the specific mitochondrial kinetics.

All different types of oscillatory behavior are obtained by varying only one parameter k_{ch}, which characterizes the activity of the ER calcium channel. In terms of mathematical description, this means that many oscillatory modes appear in a single bifurcation diagram (Fig. 3). From a biological point of view the quantity k_{ch} is appropriate for being used as a bifurcation parameter for two reasons. First, its value depends significantly on external stimuli like hormones or neurotransmitters. Therefore, k_{ch} can vary over a large scale in nature, whilst the other properties of the system (in the mathematical model: the other parameters) remain nearly unaffected. In addition, k_{ch} is accessible through experimental investigation, either by treatment of a cell with an appropriate stimulus or by directly injecting the main agonist of the channel, inositol 1,4,5-triphosphate ($InsP_3$). The second advantage of k_{ch} as bifurcation parameter lies in its role in other intra- and intercellular signaling mechanisms. Theoretical studies [15] suggest that, in some cases, the diffusion of $InsP_3$ either through the cytoplasma or through gap junctions might be a major factor of calcium signaling. Thus, in the case of calcium signaling, the response of calcium dynamics on changes of $InsP_3$ might be of elevated interest.

Bifurcation analysis shows that bursting calcium oscillations appear in various different modes. Hence, we gave special attention to the explanation of this type of oscillations in our analysis. We found that during the active phase, the model variable Ca_m declines monotonously while the remaining ones oscillate. Similar to the bifurcation analysis of Heinrich and Schuster [46], we made use of the method of two-dimensional reduction of the system, in which the 'non-active' variable is turned into a parameter. In the field of complex calcium oscillations, this has been carried out before for another model [33]. In comparison to this work, our study exhibits even more complex forms of oscillations. Besides simple limit cycles, odd- and even-folded limit cycles were also found. Birhythmicity, previously reported only for simple calcium spikes [40], has also been found

for bursting calcium oscillations. In addition, in our work trirhythmicity also appears for bursting calcium oscillations. The complexity of these coexisting limit cycles is even more expressed by the fact that they, in addition to the slight difference in their forms are, in part, also differently folded.

The most complex type of calcium oscillations found in our model is represented by chaotic bursting. In the bifurcation analysis of the model system, we studied transitions into chaotic regimes. Similar to works of Borghans et al. [33] and Houart et al. [40], we found the period doubling cascade as a typical route to chaos. In contrast to previous works, in our study the chaotic oscillations also express typical spike-like forms with reasonable amplitudes that remain nearly constant all the time. The constancy of amplitudes in the present model results from the specific role of mitochondria, which has been explained previously for simple calcium oscillations [13]. In addition to the period doubling cascade, we also found the intermittency route to chaos. Because, in all regions, the chaotic oscillations are in close proximity to intermittency-type transitions, they display a well-defined mean frequency. It should be emphasized that this well expressed frequency of the chaotic oscillations changes in dependence on the bifurcation parameter, which is related to the concentration of an extracellular agonist such as a hormone or a neurotransmitter. Therefore, all types of Ca^{2+} oscillations resulting from our model, up to the most complex chaotic bursting, exhibit the important biological feature that the external signal is encoded in terms of the temporal pattern of Ca^{2+} oscillations, the so-called frequency encoding calcium signals [3,4]. To sum up, the temporal patterns of all types of complex calcium oscillations, i.e. their spike-like forms, constant amplitudes and well defined frequencies, convincingly reproduce experimental observations [47,48].

When analyzing biological models that show chaotic behavior, it is suggestive to rise the question what particular meaning or impact that chaotic dynamics may have in living systems. Further, it might be the subject of further investigation whether there is a significant physiological difference between repetitive calcium spikes that correspond to plain limit cycle oscillations, with slight variations of amplitudes or frequencies resulting from white noise caused by external influences, and those corresponding to a mechanism that leads to chaos through intrinsic mechanisms. In another field of biology the significance of such a difference has been proven recently. The short-term variations of beat-to-beat intervals of a group of healthy persons and those with severe congestive heart failure (CHF) have been studied by Poon and Merrill [49]. These authors stated that these variations 'exhibited strongly and consistently chaotic in all healthy subjects, but were frequently interrupted by periods of seemingly non-chaotic fluctuations in patients with CHF. Chaotic data, even if discernible, exhibited a high degree of random variability over time, suggesting a weaker form of chaos. These findings suggest that cardiac chaos is prevalent in healthy heart, and a decrease in such chaos may be indicative for CHF.'

Further ideas about the physiological meaning of chaos in calcium dynamics include the possibility that chaotic systems might show different coupling properties (U. Kummer, personal communication). The trajectory of a chaotic attractor contains a range of different frequencies rather than a single one in the case of simple limit cycle. Therefore, it might be assumed that such a system is more easily adopted to external periodic perturbation. However, our first attempts to demonstrate such behavior have failed so far. For example, the coupling constant needed to synchronize cells of different oscillation frequencies could not be shown to depend on whether the systems of the uncoupled cells are in a chaotic regime. A concrete proof of this assumption is impeded by the fact that it is difficult to characterize two coupled chaotic cells as being synchronized or not synchronized, because the calcium spikes might occur simultaneously over a long time, but separately at other times.

References

[1] M. Marhl, T. Haberichter, M. Brumen, R. Heinrich, Complex calcium oscillations and the role of mitochondria and cytosolic proteins, BioSystems 57 (2000) 75–86.

[2] K.S.R. Cuthbertson, P.H. Cobbold, Phorbol ester and sperm activate mouse oocytes by inducing sustained oscillations in cell Ca^{2+}, Nature 316 (1985) 541–542.
[3] N.M. Woods, K.S.R. Cuthbertson, P.H. Cobbold, Repetitive transient rises in cytoplasmic free calcium in hormone-stimulated hepatocytes, Nature 319 (1986) 600–602.
[4] A. Goldbeter, Biochemical Oscillations and Cellular Rhythms, Cambridge University Press, Cambridge, 1996.
[5] M. Berridge, P. Lipp, M. Bootman, Calcium signalling, Curr. Biol. 9 (1999) R157–R159.
[6] T. Meyer, L. Stryer, Molecular model for receptor-stimulated calcium signalling, Proc. Natl. Acad. Sci. 85 (1988) 5051–5055.
[7] A. Goldbeter, G. Dupont, M.J. Berridge, Minimal model for signal-induced Ca^{2+} oscillations and for their frequency encoding through protein phosphorylation, Proc. Natl. Acad. Sci. 87 (1990) 1461–1465.
[8] R. Somogy, J.W. Stucki, Hormone-induced calcium oscillations in liver-cells can be explained by a simple one pool model, J. Biol. Chem. 266 (1991) 11068–11077.
[9] G. Dupont, A. Goldbeter, One-pool model for Ca^{2+} oscillations involving Ca^{2+} and inositol 1,4,5-triphosphate as co-agonist for Ca^{2+} release, Cell Calcium 14 (1993) 311–322.
[10] Y.-X. Li, J. Rinzel, Equations for $InsP_3$ receptor- mediated $[Ca^{2+}]_i$ oscillations derived from a detailed kinetic model: a Hodgekin–Huxley like formalism, J. Theor. Biol. 166 (1994) 461–473.
[11] M.S. Jafri, J. Keizer, Agonist-induced calcium waves in oscillatory cells: a biological example of Burgers equations, Bull. Math. Biol. 59 (1997) 1125–1144.
[12] M. Marhl, S. Schuster, M. Brumen, R. Heinrich, Modelling the interrelations between calcium oscillations and ER membrane potential oscillations, Biophys. Chem. 63 (1997) 221–239.
[13] M. Marhl, S. Schuster, M. Brumen, Mitochondria as an important factor in the maintainance of constant amplitudes of cytosolic calcium oscillations, Biophys. Chem. 63 (1998) 125–132.
[14] M. Marhl, S. Schuster, M. Brumen, R. Heinrich, Modelling oscillations of calcium and endoplasmic reticulum transmembrane potential. Role of signalling and buffering proteins and of the size of the Ca^{2+} sequestering ER subcompartments, Bioelectrochem. Bioenerg. 46 (1998) 79–90.
[15] T. Höfer, Model of intercellular calcium oscillations in hepatocytes: synchronization of heterogeneous cells, Biophys. J. 77 (1999) 1244–1256.
[16] M.S. Jafri, S. Vajda, P. Pasik, B. Gillo, A membrane model for cytosolic calcium oscillations. A study using Xenopus oocytes, Biophys. J. 63 (1992) 235–246.
[17] M.S. Jafri, B. Gillo, A membrane potential model with counterions for cytosolic calcium oscillations, Cell Calcium 16 (1994) 9–19.
[18] R. Rizzuto, P. Pinton, W. Carrington et al., Close contact with the endoplasmic reticulum as determinants of mitochondrial Ca^{2+} responses, Science 280 (1998) 1763–1766.
[19] L.S. Jouaville, F. Ichas, E.L. Holmuhamedov, P. Camacho, J.D. Lechleiter, Synchronization of calcium waves by mitochondrial substrates in *Xenopus laevis* oocytes, Nature 377 (1995) 438–441.
[20] S. Hehl, A. Gollard, B. Hille, Involvement of mitochondria in intracellular calcium sequestration by rat gonadotropes, Cell Calcium 20 (1996) 515–524.
[21] D.F. Babcock, J. Herrington, P.C. Goodwin, Y.B. Park, B. Hille, Mitochondrial participation in the intracellular Ca^{2+} network, J. Cell Biol. 136 (1997) 833–844.
[22] V.A. Golovina, M.P. Blaustein, Spatially and functionally distinct Ca^{2+} stores in sarcoplasmic and endoplasmic reticulum, Science 275 (1997) 1643–1648.
[23] D.F. Babcock, B. Hille, Mitochondrial oversight of cellular Ca^{2+} signalling, Curr. Opin. Neurobiol. 8 (1998) 398–404.
[24] L.S. Jouaville, F. Ichas, J.-P. Mazat, Modulation of cell calcium signals by mitochondria, Mol. Cell. Biochem. 184 (1998) 371–376.
[25] S. Ricken, J. Leipziger, R. Greger, R. Nitschke, Simultaneous measurements of cytosolic and mitochondrial Ca^{2+} transients in HT29 cells, J. Biol. Chem. 273 (1998) 34961–34969.
[26] P.B. Simpson, J.T. Russell, Role of mitochondrial Ca^{2+} regulation in neuronal and glial cell signalling, Brain Res. Rev. 26 (1998) 72–81.
[27] P.B. Simpson, J.T. Russell, Mitochondrial Ca^{2+} uptake and release influence metabotrobic and ionotropic cytosolic Ca^{2+} responses in rat oligodendrcyte progenitors, J. Physiol. 508 (1998) 413–426.
[28] P.B. Simpson, S. Mehotra, D. Langley, C.A. Sheppard, J.T. Russel, Specialized distributions of mitochondria and endoplasmic reticulum proteins define Ca^{2+} wave amplification sites in cultured astrocytes, J. Neurosci. Res. 52 (1998) 672–683.
[29] A.J. Verkhratcky, O.H. Petersen, Neuronal calcium stores, Cell Calcium 24 (1998) 333–343.
[30] R.M. Drummond, R.A. Tuft, Release of Ca^{2+} from the sarcoplasmic reticulum increases mitochondrial $[Ca^{2+}]$ in rat pulmonary artery smooth muscle cells, J. Physiol. 516 (1999) 139–147.
[31] G. Magnus, J. Keizer, Minimal model of β-cell mitochondrial Ca^{2+} handling, Am. J. Physiol. (Cell Physiol. 42) 273 (1997) C717–C733.
[32] V.A. Selivanov, F. Ichas, E.L. Holmuhamedov, L.S. Jouaville, Y.V. Evtodienko, J.-P. Mazat, A model of mitochondrial Ca^{2+}-induced Ca^{2+} release stimulating the Ca^{2+} oscillations and spikes generated by mitochondria, Biophys. Chem. 72 (1998) 111–121.
[33] J.A.M. Borghans, G. Dupont, A. Goldbeter, Complex intracellular calcium oscillations. A theoretical exploration of possible mechanisms, Biophys. Chem. 66 (1997) 25–41.
[34] T.R. Chay, Electrical bursting and luminal calcium oscil-

lation in excitable cell models, Biol. Cybern. 75 (1996) 419–431.
[35] G. de Vries, Multiple bifurcations in a polynomal model of bursting oscillations, J. Nonlinear Sci. 8 (1998) 281–316.
[36] C.C. Canavier, J.W. Clark, J.H. Byrne, Simulation of the bursting activity of neuron R15 in Aplysia: role of ionic currents, calcium balance, and modulatory transmitters, J. Neurophysiol. 66 (1991) 2107–2124.
[37] R.J. Butera, Jr., Multirhythmic bursting, Chaos 8 (1997) 274–284.
[38] J. Rinzel, Y.S. Lee, Dissection of a model for neuronal parabolic bursting, J. Math. Biol. 25 (1987) 653–675.
[39] P. Shen, R. Larter, Chaos in intracellular Ca^{2+} oscillations in a new model for non-excitable cells, Cell Calcium 17 (1995) 225–232.
[40] G. Houart, G. Dupont, A. Goldbeter, Bursting, chaos and birhythmicity originating from self-modulation of the inositol 1,4,5-triphosphate signal in a model for intracellular Ca^{2+} oscillations, Bull. Math. Biol. 61 (1999) 507–530.
[41] U. Kummer, L.F. Ohlsen, C.J. Dixon, A.K. Green, E. Bornberg-Bauer, G. Baier, Switching from simple to complex oscillations in calcium signalling, Biophys. J. 79 (2000) 1188–1195.
[42] L.F. Olsen, U. Kummer, A.K. Green, C.J. Dixon, M.J.B. Hauser, Dynamics and information processing in biochemical pathways, in: E. Bornberg-Bauer et al. (Ed.), Proceedings Workshop on Computation of Biochemical Pathways and Genetic Networks, Heidelberg, 1999.
[43] F. Ichas, L.S. Jouaville, S.S. Sidash, J.-P. Mazat, E.L. Holmuhamedov, Mitochondrial calcium spiking: a transduction mechanism based on calcium-induced permeability transition involved in cell calcium signalling, FEBS Lett. 348 (1994) 211–215.
[44] F. Ichas, L.S. Jouaville, S.S. Sidash, J.-P. Mazat, E.L. Holmuhamedov, Mitochondrial calcium spiking: the physiological face of permeability transition? in: E. Gnaiger et al. (Ed.), Modern Trends in BioThermoKinetics 3, Innsbruck Univ. Press, Innsbruck, 1994.
[45] J. Rinzel, E. Teramoto, M. Yamaguti (Eds.), Mathematical Topics in Population Biology, Morphogenesis and Neurosciences, Vol. 71, Lecture Notes in Biomathematics, Springer, Berlin, 1987, 267
[46] R. Heinrich, S. Schuster, The Regulation of Cellular Systems, Chapman & Hall, New York, 1996.
[47] A.K. Green, C.J. Dixon, A.G. McLenan, P.H. Cobbold, M.J. Fisher, Adenine dinucleotide-mediated cytosolic free Ca^{2+} oscillations in single hepatocytes, FEBS 322 (1993) 197–200.
[48] I. Marrero, A. Sanchez-Bueno, P.H. Cobbold, C.J. Dixon, Taurolitocholate and taurolitocholate 3-sulfate exert different effects on cytosolic free Ca^{2+} concentration in rat hepatocytes, Biochem. J. 300 (1994) 383–386.
[49] C.-S. Poon, C.K. Merrill, Decrease of cardiac chaos in congestive heart failure, Nature 389 (1997) 492–495.